γ-ray polarization in transmission through a noncubic and nonmagnetic single crystal

P. Boolchand, W. Bresser, G. Anaple, and Y. Wu
Department of Electrical and Computer Engineering, University of Cincinnati, Cincinnati, Ohio 45221-0030

R. N. Enzweiler
Department of Physics and Geology, Northern Kentucky University, Highland Heights, Kentucky 41099

R. Coussement
Katholieke Universiteit Leuven, 3001 Leuven, Belgium

J. Grover
Department of Geology, University of Cincinnati, Cincinnati, Ohio 45221-0013

(Received 7 March 1994)

A Mössbauer-effect experiment, with γ-ray wave vector $\mathbf{k}$ directed both along and normal to the c axis of a siderite ($FeCO_3$) single-crystal platelet, has been systematically performed in the temperature range $50 < T < 300$ K. The T dependence of the integrated area $S(T)=S_\pi(T)+S_\sigma(T)$ under the quadrupole doublet reveals that at 300 K the Debye-Waller factors are $f_c=0.72(2)$ and $f_{\perp c}=0.75(2)$. Independently, the area ratios S_π/S_σ under the π and σ quadrupole components, measured at 300 K, confirm the lack of a spatial anisotropy of the f factor but, more significantly, confirm the theoretically predicted polarization-dependent resonant-absorption cross section in transmission through the crystal.

I. INTRODUCTION

The mineral siderite ($FeCO_3$) has the calcite structure, rhombohedral space group $R\bar{3}c$, in which the c axis (optic axis) possesses threefold rotational symmetry. The Fe^{2+} cation in this structure is subject to a large electric-field gradient (EFG), and this results in a well-resolved quadrupolar doublet that characterizes the room-temperature Mössbauer effect spectrum of this material.[1-3] Point-group symmetry considerations require the EFG in siderite to be axially symmetric [$\eta=(V_{xx}-V_{yy})/V_{zz}=0$]; the EFG tensor can thus be completely specified by V_{zz} alone.

Nearly a quarter of a century ago, Goldanski *et al.*[4] examined the area ratio $S_\pi/S_\sigma(\theta)$ of the π ($\pm\frac{3}{2}\rightarrow\pm\frac{1}{2}$) and σ ($\pm\frac{1}{2}\rightarrow\pm\frac{1}{2}$) quadrupole components as a function of crystal orientation θ, measured with respect to the c axis, and claimed a rather large spatial anisotropy ($f_c/f_{\perp c}>3$) of the Lamb-Mössbauer factor (f factor) in siderite. These claims were disputed by Housley, Gonser, and Grant,[5] who recognized that in their analysis Goldanski *et al.*[4] did not include fractional polarization of the quadrupole components. When included in the theory of resonant absorption, the fractional polarization of the quadrupole components can alter the thickness dependence of the measured area ratio S_π/S_σ qualitatively for γ-ray propagation along certain crystal directions. The direction $\theta=\pi/2$, corresponding to the γ-ray wave vector $\mathbf{k}\perp c$ axis, happens to be one along which pronounced polarization effects occur. The transmitted γ beam becomes partially polarized in this direction, and area ratio S_π/S_σ becomes more or less independent of effective absorber thickness ($x=n\sigma_0 f$) at $x>5$.

The work of Housley, Grant, and Gonser[6] on the coherence and polarization effects of γ radiation in transmission through single crystals was well ahead of its times. Their theory provides a means to establish the degree of γ-ray polarization by measuring the area ratio S_π/S_σ, and this is of current interest in the field of γ optics. In an attempt to verify the theory, Housley, Gonser, and Grant[5] performed area-ratio S_π/S_σ measurements at $\theta=\pi/2$ for a siderite single-crystal sample. They found the observed ratio to be somewhat larger than their theoretical predictions,[5] and this indicated less polarization of the transmitted beam than expected theoretically. Housley, Gonser, and Grant[5] attributed this deviation to the presence of impurities in their mineral sample. Nevertheless, they concluded that the spatial anisotropy of the f factor, if any, was likely to be small.

A direct and more accurate method to measure f factors is through T dependence of the integrated area $S(T)=S_\pi(\theta,T)+S_\sigma(\theta,T)$ in a Mössbauer effect experiment. We also came to recognize that such experiments, at any angle θ in the range $0\le\theta\le\pi/2$, can be performed with one $FeCO_3$ single-crystal absorber, provided it is cut parallel to the cleavage plane and suitably oriented. We have performed such experiments and have measured the f factors for our $FeCO_3$ single-crystal sample, and obtained $f_c=0.72(2)$ for $\mathbf{k}\|c$ axis and $f_{\perp c}=0.75(2)$ for $\mathbf{k}\perp c$ at 300 K. This helps resolve the controversy on the f factors in $FeCO_3$ in favor of the work of Housley, Gonser, and Grant.[5] But more significantly, by measuring f factors directly, we have established the effective absorber thickness $x_\parallel$ and $x_\perp$ of our single-crystal sample for $\mathbf{k}\|c$ and $\mathbf{k}\perp c$ rather precisely. From a measurement of the area ratio S_π/S_σ at $\theta=\pi/2$ and the effective ab-

0163-1829/94/50(10)/6833(7)/$06.00

sorber thickness ($x_\perp$) of our single-crystal sample, we have been able quantitatively to confirm the theory of Housley, Gonser, and Grant.[5] Our work thus provides an experimental confirmation of the theory of γ-ray polarization in transmission through a nonmagnetic and noncubic crystal, using area ratios of the quadrupole components as a polarimeter in Mössbauer spectroscopy.

II. EXPERIMENTAL DETAILS

A. Characterization of siderite

Our siderite sample comes from the cryolite locality of Ivigtut, Greenland. It is light greenish yellow in color and cleaves perfectly on the $\{10\bar{1}4\}$ faces. (We use here the structural cell rather than the conventional morphologic cell.) It was characterized by x-ray Laue back reflection and powder diffraction, chemical analysis, and dc magnetometry. The Laue back-reflection patterns displayed sharp spots indicative of the good single-crystal character of our sample. The x-ray lattice parameters were measured using both a Siemens D-500 and a Rigaku powder diffractometer and found to be $a=4.6930(5)$ Å and $c=15.377(3)$ Å. Figure 1 displays a θ-2θ scan of our siderite sample. These parameters are strikingly close to those [$a=4.6935(2)$ Å, $c=15.3860(8)$ Å] known[7] for other siderite samples from Ivigtut, Greenland. The published[8] chemical analysis of such samples reveals 2.86 wt. % Mn and 0.20 wt. % Mg as the principal nonstoichiometric components (0.09 Mn atoms and 0.01 Mg atoms for every two Fe^{2+} cations). We have confirmed that Mn^{2+} is present in our sample by means of inductively coupled plasma (ICP) optical spectroscopy. It is worthwhile to note that the lattice parameters reported by Sharp[9] for pure synthetic $FeCO_3$ are $a=4.690$ Å and $c=15.370$ Å, quite close to those of our sample. This suggests that the chemical purity of siderite samples from Ivigtut, Greenland is in rather good accord with our ICP analysis. Using an EG&G-PAR vibrating-sample magnetometer, we measured the T dependence of the magnetic susceptibility $\chi(T)$ and observed a cusp at $T_N=39.3(5)$ K

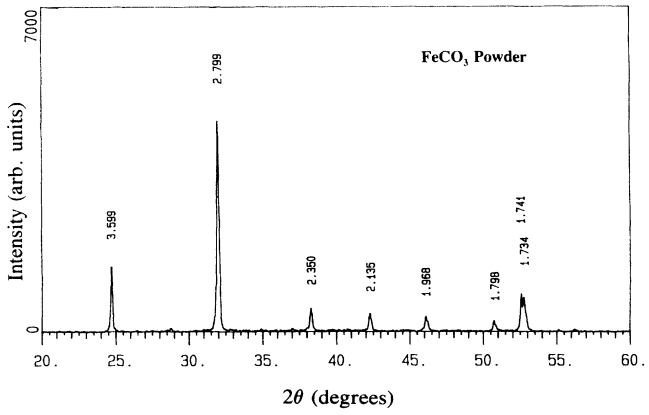

FIG. 1. X-ray θ-2θ scan of $FeCO_3$ taken with a Rigaku D-2000 powder diffractometer displaying peaks of the rhombohedral phase. The peaks are a close match to the JCPDS file No. 29-696 identified with siderite from Ivigtut, Greenland.

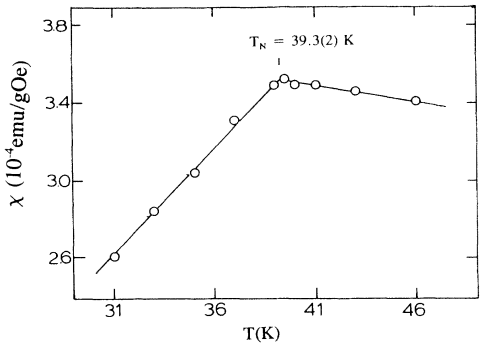

FIG. 2. Magnetic susceptibility $\chi(T)$ of $FeCO_3$ as a function of temperature displaying a cusp at the Néel temperature $T_N=39.3(2)$ K.

(see Fig. 2), which we identify as the antiferromagnetic transition temperature of our siderite sample. Okiji and Kanamori[3] established the Néel temperature of a synthetic $FeCO_3$ sample at $T_N=38.3$ K by Mössbauer-spectroscopy measurements.

B. Preparation and mounting of the $FeCO_3$ single-crystal absorber

We cleaved $a\sim\frac{1}{2}$ mm thick platelet of 1.2×1.2 cm^2 area from the siderite crystal. The platelet was polished on both sides and mounted for support on a thin silica flat reduced in thickness to $148\pm(10)$ μm using a grinding wheel. The thickness of the sample was optically verified using a Nikon microscope. Supporting the sample on an optically transparent flat served both to inhibit chipping the sample with grinding and to facilitate optical alignment of the crystal. The angle between the optic axis and the cleavage plane $\{10\bar{1}4\}$ was next calculated to be 46.6° from the measured lattice parameters; the y-z plane [see Fig. 3(a)] containing the optic axis was identified using a polarizing microscope.

As illustrated in Fig. 4, the free surface of the sample (S) was next supported on a thin 0.005-in Be disk (B) with a thermally conducting vanish. The Be disk was mounted on a specially designed oxygen-free high-purity

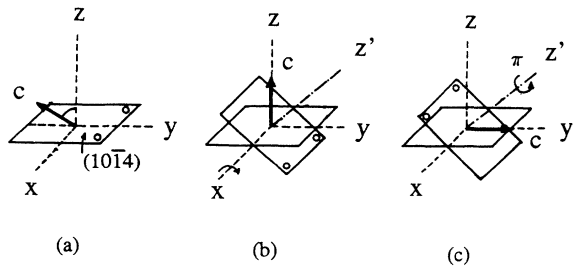

FIG. 3. The figure schematically illustrates (a) direction of the c axis making an angle $\pi/2$-α with respect to an $FeCO_3$ single-crystal platelet (xy), (b) rotation of the platelet by $\alpha=46°$ about the x axis brings the c axis perpendicular to the y axis, while in (c) a rotation of the sample by π about the normal to the platelet (z') brings the c axis prallel to the y axis. In our experiments the γ-ray wave vector **k** is along the y axis.

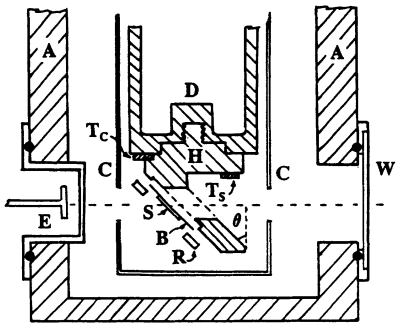

FIG. 4. Experimental setup used for T-dependent Mössbauer-effect experiments on $FeCO_3$: The single-crystal sample (S) varnished on to a Be disk (B) is mounted on a Cu holder (H) with a Cu ring (R) and In gaskets (not shown). The holder H is screwed into the cold finger (D) of a He closed-cycle cryostat. The finger D is mechanically isolated from the cold head (not shown) and cooled by He exchange gas. The radiation shield (C) and Al vacuum shroud (A) provide isolation of the cold stage from ambient. The temperature of the sample is measured by a Si diode (T_s) anchored to the holder H, while the temperature control of the assembly is achieved by a heater and a control Si-diode sensor (T_c). The Mössbauer emitter (E) at room temperature moves to and fro along the horizontal axis and the transmitted γ radiation through the absorber S detected by a proportional counter (not shown) at the far end.

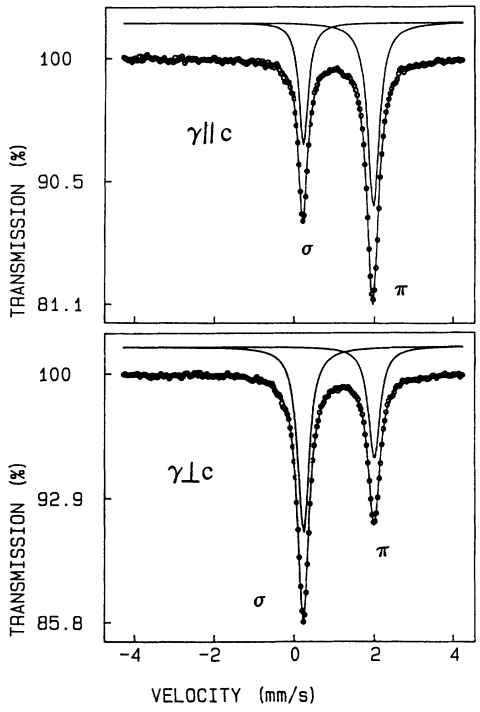

FIG. 5. Room-temperature Mössbauer spectra of an $FeCO_3$ single crystal for γ-ray wave vector $\mathbf{k}\|c$ axis (top) and $\mathbf{k}\perp c$ axis (bottom).

(OFHP) Cu sample holder (H) with In O-ring gaskets (not shown in Fig. 4) and a Cu clamping ring (R). This arrangement was found sufficient to achieve intimate thermal contact between the sample and cold finger for T-dependent experiments. The Cu surface on which the Be disk was supported made an angle $\alpha \simeq 47°$ with the vertical axis (Fig. 4). This permitted the γ-ray wave vector $\mathbf{k}$ to be oriented perpendicular to the c axis [Fig. 3(b)]. The Cu holder was screwed into a cold finger (D) of a DMX-20 He closed-cycle cryostat from APD, Inc. We have previously shown[10] that this closed-cycle system, when suitably mounted, is vibration free so that there is no line broadening on the inner two lines of α-Fe. To obtain the $\mathbf{k}\|c$-axis geometry, the Be disk was merely rotated by π on its supported surface, as illustrated in Fig. 3(c).

C. Mössbauer-effect methodology and results

The principal results of our work appear in Figs. 5–7. The spectra were recorded in a 512-channel analyzer using an MCS-II PC card from Oxford Instruments. A 10-mC ^{57}Co source in Rh metal was used as an emitter and the γ rays detected in a 2-atm-filled Kr proportional counter. Typical spectra obtained at room temperature are displayed in Fig. 5. These were fitted to two Lorentzian line shapes using least-squares methods with no restrictions on line positions, intensities, and full widths at half maximum (Γ). The room-temperature Mössbauer parameters of our $FeCO_3$ sample reveal an isomer shift $\delta = 1.002(4)$ mm/s relative to α-Fe and a quadrupole splitting of 1.770(4) mm/s. Table I provides a summary of the area-ratio $S_\pi/S_\sigma(\theta)$ results. The T dependence of the integrated area (S_π/S_σ) under the resonance is shown in Fig. 6. In this figure the solid curve through the data points is a least-squares fit of the integrated area to a Debye density of vibrational states. This yields an effective Debye temperature $\theta_D = 359(7)$ for $\mathbf{k}\|c$ axis and a $\theta_D = 386(8)$ for $\mathbf{k}\perp c$ axis. Given these vibrational temperatures, we obtain f factors at 300 K of

$$f_c = 0.72(2), \quad f_{\perp c} = 0.75(2) .$$

The present results yield no measurable spatial anisotropy of the Debye-Waller factor in our $FeCO_3$ sample, and this is a point we will discuss comprehensively in the next section. Given these Debye-Waller factors, we have calculated the effective absorber thickness x of our sample as follows. We have taken the thickness of our platelet tilted at 43.4° with respect to the vertical axis at 148

TABLE I. Area ratio S_π/S_σ deduced from observed intensity (I) and linewidth (Γ) for the π and σ quadrupole components for γ-ray wave vector $\mathbf{k}\|c$ axis ($\theta = 0$) and $\mathbf{k}\perp c$ axis ($\theta = \pi/2$).

	I_π (%)	Γ_π (mm/s)	I_σ (%)	Γ_σ (mm/s)	S_π/S_σ
$\theta = 0$	18.87(8)	0.344(4)	12.50(9)	0.285(3)	1.83(2)
$\theta = \pi/2$	8.39(4)	0.354(4)	14.19(8)	0.357(3)	0.586(3)

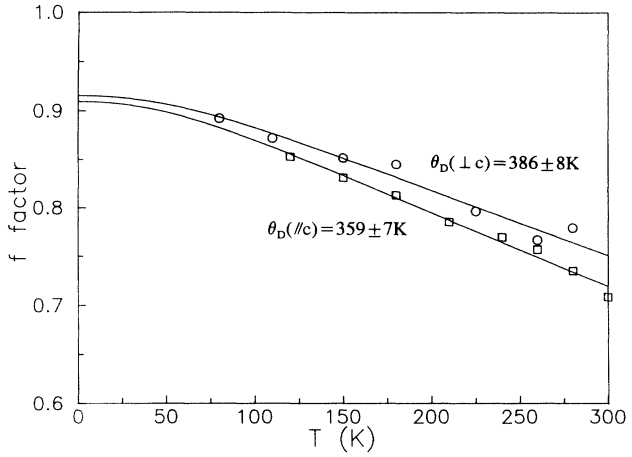

FIG. 6. T dependence of the integrated area $S_T(T)$ under the nuclear resonance for γ-ray wave vector $\mathbf{k}\|c$-axis (□) and $\perp c$ axis (○) of a single-crystal $FeCO_3$ absorber. The solid lines are a least-squares fit of the data points to a Debye density of states yielding indicated Debye temperatures.

$\mu/\cos 43.4°$, the density of $FeCO_3$ at 3.93 g/cm^3, and obtain the number of ^{57}Fe nuclei/cm^2, $n=8.48\times10^{18}$, after correcting for Mn and Mg cation impurities in the crystal sample. Taking the maximum resonant cross section $\sigma_0=2.57\times10^{-18}$ cm^2 and $f_c=0.72(2)$, we obtain $x_\parallel=15.7(6)$. Since the f factor and absorber thickness for the $\theta=\pi/2$ geometry is nearly the same as the one for the $\theta=0$ geometry, the effective absorber thickness $x_\perp$ for $\mathbf{k}\perp c$ axis is found to be nearly the same [16.3(7)].

III. DISCUSSION

In our discussion, we will focus on two specific issues, one related to the interpretation of the measured area ratios S_π/S_σ, and the second on the spatial isotropy of the recoil-free fraction (f factor) in siderite.

A. Angular distributions and sign of quadrupole interaction

The origin of the electric in $FeCO_3$ has been the subject of several earlier publications.[1–3] The positive sign of e^2qQ is traced to an orbital doublet as the ground state of the Fe^{2+} ion in a rhombic crystal field. This means that the π transition ($\pm\frac{1}{2}\rightarrow\pm\frac{3}{2}$) has a higher energy than the σ transition ($\pm\frac{1}{2}\rightarrow\pm\frac{1}{2}$), and in the spectrum the π transition appears at a more positive velocity than the σ transition, as shown in Fig. 5. The single-crystal results presented here and elsewhere[4,5] unequivocally support the positive sign of e^2qQ through the measured area ratios $S\pi/S\sigma$. For $\mathbf{k}\|c$ axis (i.e., $\theta=0$), in the thin-absorber approximation ($x_\parallel<1$) one expects $S_\pi/S_\sigma=c_\pi/c_\sigma=3$ from the angular distributions $c(\theta)$ of the π and σ quadrupole components,[4,5]

$$c_\pi(\theta)=[\tfrac{1}{2}+\tfrac{1}{8}(3\cos^2\theta-1)]x\ , \tag{1}$$

$$c_\sigma(\theta)=[\tfrac{1}{2}-\tfrac{1}{8}(3\cos^2\theta-1)]x\ , \tag{2}$$

while for $\mathbf{k}\perp c$ axis (i.e., $\theta=\pi/2$), on the other hand, in the thin-absorber approximation ($x_\perp<1$), one expects $=c_\pi/c_\sigma=\frac{3}{5}$ from Eqs. (1) and (2). At the outset, one can clearly observe $S_\pi/S_\sigma>1$ for $\mathbf{k}\|c$ axis, while $S_\pi/S_\sigma<1$ for $\mathbf{k}\perp c$ axis from the spectra of Fig. 5. The sense of the asymmetries in the area ratios unequivocally supports a positive sign of the quadrupole coupling in $FeCO_3$. To understand these S_π/S_σ results quantitatively in a crystal of finite thickness is a more formidable task, as we discuss next.

B. γ-ray transmission through a single crystal of finite thickness

In considering transmission of an incident γ ray of some polarization from a source through a single-crystal absorber of finite thickness, in general, the polarization of the radiation transmitted in the forward direction will be different from that of the incident beam. This is largely because the reemitted radiation from the first layer of nuclei in the absorber (after resonant absorption has occurred) will have a polarization different from that of the incident radiation. In a single-crystal absorber, one must coherently add contributions to the resonant-absorption amplitude of each successive layers of nuclei in the crystal with due consideration to the changing polarization. The index of refraction of the absorber medium can in general be described in terms of a 2×2 density matrix[11,12] corresponding to the two possible independent states of polarization of the radiation. Mathematically, the transmission requires a calculation of the complex index of refraction, with the real part describing polarization changes, while the imaginary part represents the nuclear resonant absorption. The complex index of refraction, n, can be written[11,12] in terms of $F(\mathbf{k},\mathbf{k}')$, the coherent forward scattering amplitude, as follows:

$$n=1+(2\pi N/k^2)F(\mathbf{k},\mathbf{k}')\ , \tag{3}$$

where $\mathbf{k}$ and $\mathbf{k}'$ are the wave vectors of incident and scattered radiation, and N the number of nuclei/cm^3. For γ propagation along specific crystal directions along which the refractive-index matrix becomes diagonal, one can calculate the transmission by regarding the incident γ beam to be made up of two components, with polarizations corresponding to the basic polarization in which n is diagonal.

1. γ-ray $\mathbf{k}$ parallel to the c axis

As discussed by Housley, Gonser, and Grant,[5,6] when $\mathbf{k}$ is parallel to the trigonal axis of $FeCO_3$, the refractive-index matrix is diagonal in a basis of right and left-handed circular polarizations and the fractional polarizations $a=[(\rho_{11}-\rho_{22})/(\rho_{11}-\rho_{22})]$ of the π and σ quadrupole components are zero, as seen by requiring $\theta=0$ in the equations[5,6]

$$a_\pi(\theta)=\frac{\sin^2\theta}{1+\cos^2\theta}\ , \tag{4}$$

$$a_\sigma(\theta)=\frac{3\sin^2\theta}{5-3\cos^2\theta}\ . \tag{5}$$

In writing Eqs. (4) and (5) we have taken the asymmetry parameter (η) of the EFG to be zero. The thickness dependence of the observed area ratio S_π/S_σ for the case of an absorber of effective thickness x reduces to the expression

$$\frac{S_\pi}{S_\sigma}=\frac{c_\pi e^{-c_\pi/2}[I_0(c_\pi/2)+I_1(c_\pi/2)]}{c_\sigma e^{-c_\sigma/2}[I_0(c_\sigma/2)+I_1(c_\sigma/2)]} \tag{6}$$

used to describe[5,6] saturation effects associated with an unpolarized γ-ray beam. In Eq. (6), I_0 and I_1 represent Bessel functions of imaginary assignments. Figure 7(a) shows a plot of Eq. (6) as a function of x. In the thin-absorber limit as $x\to 0$, the area ratio $S_\pi/S_\sigma\to 3$. With increasing x, the area ratio S_π/S_σ decreases systematically as shown in Fig. 7(a) and saturates at a value of about 1.75 as $x>15$. For the measured area ratio S_π/S_σ and the effective absorber thickness $x_\parallel$, our data point in Fig. 7(a) lies nicely on the theoretical curve.

2. *γ-ray wave vector* **k** *perpendicular to the c axis*

For γ-ray propagation normal to the c axis, the situation is qualitatively different, however. Both the π and σ components are now fractionally polarized with $a_\pi=1$ and $a_\sigma=0.6$ as determined by substituting $\theta=\pi/2$ in Eqs. (4) and (5). Housley, Gonser, and Grant[5,6] demonstrated that in this instance one can view the unpolarized γ ray from the source to be polarized into two components of equal intensity with polarizations parallel and normal to the partial polarizations of the π and σ quadrupole components. The thickness dependence of the area ratio S_π/S_σ can now be obtained by calculating the contributions to the area for the two polarizations separately and then adding these contributions together:

$$S=\frac{1}{2}c(1+a)e^{-c(1+a)/2}\left\{I_0\left[\frac{c}{2}(1+a)\right]+I_1\left[\frac{c}{2}(1+a)\right]\right\}+\frac{1}{2}c(1-a)e^{-c(1-a)/2}\left\{I_0\left[\frac{c}{2}(1-a)\right]+I_1\left[\frac{c}{2}(1-a)\right]\right\}. \tag{7}$$

In Fig. 7(b), the solid line shows the thickness dependence of the area ratio S_π/S_σ calculated[5,6] from Eq. (7). For comparison we also show in Fig. 7(b), with a dashed line, the expected S_π/S_σ (x) dependence when no polarization effects are taken into account, i.e., $a_\pi=a_\sigma=0$. For this case, Eq. (7) reduces to Eq. (6). The qualitative difference between these two curves highlights the crucial role played by partial polarizations of the π and σ quadrupole components in changing the thickness saturation behavior of the area ratio.[5]

Our measured area ratio S_π/S_σ (Table I) and the effective absorber thickness $x_\perp$ are projected in Fig. 7(b) for $\mathbf{k}\perp c$ axis. In projecting our experimental results in Fig. 7, we would like to emphasize that values for both the abscissa and the ordinate were experimentally determined with no adjustable parameters. Specifically, the area ratio S_π/S_σ was deduced directly from the spectra shown in Fig. 5 by deconvoluting the line shape. The effective absorber thickness $x_\perp$ was calculated from the physical thickness and the room-temperature f factor ($f_{\perp c}$) established independently from the T-dependent measurements alluded to earlier (Fig. 6). We estimate the uncertainty in the area-ratio measurement at $\sim 1\%$, to reflect primarily the statistical quality and reproducibility of the data. To achieve this accuracy, we accumulated 10^6 counts per channel in a run and repeated the measurement three times to ascertain reproducibility. The uncertainty in the effective absorber thicknesses $x_\perp$ or $x_\parallel$ derives primarily from the uncertainty of the physical thickness of the $FeCO_3$ crystal; given our polishing and thinning technique, we estimate this to be about 10%. It is clear from Fig. 7(b) that the present experimental results agree rather well with the predicted calculations of the area ratio provided fractional polarization of the

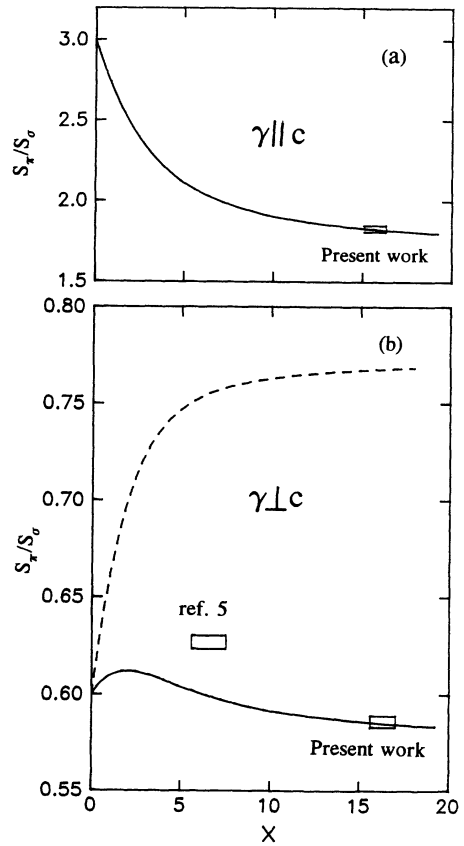

FIG. 7. Area ratio S_π/S_σ for γ-ray wave vector (a) $\mathbf{k}\parallel c$ axis and (b) $\mathbf{k}\perp c$ axis along with observed data points. The solid line is the theoretically expected variation of S_π/S_σ as a function of effective absorber thickness x. In the bottom panel, the dashed curve illustrates the expected behavior for the case when the fractional polarization of the π and σ quadrupole components is taken to be zero. The result of Housley, Gouser, and Grant taken from Ref. 5 is also projected for comparison with present results.

quadrupole components is explicitly considered.

We have also projected in Fig. 7(b) the experimental determination for $\mathbf{k}\perp c$ axis obtained by Housley, Gonser, and Grant.[5] The difference between the present result and the result of Housley, Gonser, and Grant,[5] we believe, reflects primarily chemical differences in the make-up of the two mineral samples used. Housley, Gonser, and Grant.[5] noted that their siderite sample contained 10 at. % of Mg impurities. Perusal of the standard mineral literature[8] on siderite shows that there are two well-known and documented sources of this mineral in which Fe^{2+} is replaced by ~ 10 at. % Mg cation (Styria, Austria and Telemarken, Norway). Siderite from both these locales also contains a substantial amount of Mn impurities, the former 4 at. % and the latter 6 at. %. It is thus not surprising that Housley, Gonser, and Grant.[5] were unable to get quantitative confirmation on the theory from their mineral sample because the presence of those impurities may destroy some of the coherent forward scattering. Goldanskii *et al.*[4] obtained an area ratio S_π/S_σ of 0.68(3) at $\theta=\pi/2$, for their 240-μm-thick siderite sample. Given our measured f factor ($f_{\perp c}$), we estimate an upper limit to the effective absorber thickness $x_\perp$ of 32.7 for the sample of Goldanskii *et al.*[4] Naturally, if there are Mg and/or Mn cation impurities in the sample, the Fe effective absorber thickness $x_\perp$ will decrease proportionately from 32.7. Since there is no information available in Ref. 4 on sample characterization, particularly purity, we are unable objectively to obtain $x_\perp$ for their sample. In any event, the observed S_π/S_σ obtained by Goldanski *et al.*[4] is much too large for any reasonable value of $x_\perp$ to be compatible with the theory of Housley, Gonser, and Grant,[5] and this broadly raises the question of purity of the mineral sample available to these workers.

In summary, the measured area ratios S_π/S_σ presently obtained on siderite for $\mathbf{k}\parallel c$ axis and $\mathbf{k}\perp c$ axis are quantitatively compatible with the theory of Housley, Gonser, and Grant.[5] and provide clear experimental confirmation of the ideas developed to understand γ-ray resonant absorption in transmission through thick single crystals.

IV. SPATIAL ANISOTROPY OF THE f FACTOR IN SIDERITE

Our results on the T dependence of the f factor shown in Fig. 6 show that $f_c \simeq f_{\perp c}$, in sharp contrast to the conclusions of Goldanskii *et al.*[4] This deserves comment. The near equality of f_c and $f_{\perp c}$ is independently confirmed both by the T dependence of the partial areas $S_\pi(T)$ and $S_\sigma(T)$ and by the observed area ratios S_π/S_σ shown in Fig. 7. If one extracts the values of $x_\parallel$ and $x_\perp$ that would best fit the observed S_π/S_σ at $\theta=0$ and $\pi/2$ by drawing a horizontal line in Figs. 7(a) and 7(b) and noting the intersection of this line with the theoretical curves, one finds $x_\parallel \simeq x_\perp$. Since the physical thickness of the sample used in measurements along the two directions are the same, it inevitably follows that $f_c \simeq f_{\perp c}$.

In the calcite structure, the cleavage plane $\{10\bar{1}4\}$ makes an angle of 46° with the c axis. One would thus predict interatomic forces along $\theta=46°$ to be weak and the f factor, if anything, to display a local minimum along this direction. Since this direction resides midway between the c axis ($\theta=0$) and the a axis ($\theta=\pi/2$), the near equality of $f_c \simeq f_{\perp c}$ is just the expected result.

Finally, it is also unlikely that any reduction in the f factor along $\theta=46°$ would affect the observed area ratios S_π/S_σ either in a single crystal or in a polycrystalline sample to any significant manner. The angular distributions of the π and σ quadrupole components are emitted preferentially[13] along the c axis and a axes, respectively. Neither of these angular distributions is peaked at an angle midway between $\theta=0$ and 90° so as to probe lattice vibrations along the cleavage planes sensitively. For these reasons the choice of $FeCO_3$ as a host, to test of the spatial anisotropy of lattice vibrations[4] quantitatively, is thus somewhat unfortunate.

V. CONCLUDING REMARKS

We have systematically examined the T dependence of the Mössbauer effect in the range $50 < T < 300$ K for a γ-ray wave vector $\mathbf{k}$ parallel and perpendicular to the c axis of rhombohedral $FeCO_3$ single crystals. The results show that the f factor along the c axis, $f_c=0.72(2)$, and that perpendicular to the c axis, $f_{\perp c}=0.75(2)$, are almost the same. More significantly, the measured area ratios S_π/S_σ under the quadrupole components and the measured effective absorber thicknesses x for both $\theta=0$ and $\pi/2$ directions are quantitatively consistent with (a) an axially symmetric $\eta=0$ electric-field gradient, (b) lack of fractional polarization of the quadrupole components along the c axis, and (c) the existence of a fractional polarization $a_\pi=1$ and $a_\sigma=0.6$ of the quadrupole components perpendicular to the c axis. These results provide quantitative confirmation of the theory of Housley, Gonser, and Grant,[5] advanced 25 years ago to describe coherence and polarization effects in Mössbauer transmission experiments through a nonmagnetic and noncubic single crystal.

In a forthcoming paper, we will examine Mössbauer-effect results in siderite at $T < T_N$. In the antiferromagnetic phase, the magnetic hyperfine field at Fe can be temperature tuned to satisfy a condition for level crossing of the pair of Zeeman levels $|m=-\frac{3}{2}\rangle$ and $|m=+\frac{1}{2}\rangle$ of the first excited state in ^{57}Fe. This has also been observed. To analyze the line shapes quantitatively, particularly the size of the resonant effect at the nuclear level crossing, a reliable knowledge of the Debye-Waller factors and asymmetry parameter η of the EFG is necessary. These parameters have now been established for our sample from the present work.

ACKNOWLEDGMENTS

We acknowledge with pleasure the assistance provided by Geni Edwards and Doug Bolling in the fabrication of $FeCO_3$ samples, and Min Zhang in the analysis and plots of the results, and Dr. Richard Burrows with the ICP measurements. It is a pleasure to acknowledge discussions with B. Goodman on the basic science issues addressed here. This work was supported by the Ballistic Missile Defense Organization and managed through ONR Grant No. N00014-88-K-2035.

[1]K. Ono and A. Ito, J. Phys. Soc. Jpn. **19**, 899 (1964).
[2]A. Okiji and J. Kanamori, J. Phys. Soc. Jpn. **19**, 908 (1964).
[3]Hang Nam Ok, Phys. Rev. **185**, 475 (1969).
[4]V. I. Goldanski, E. F. Makarov, I. P. Suzdalev, and I. A. Vinogradov, Phys. Rev. Lett. **20**, 137 (1968).
[5]R. M. Housley, U. Gonser, and R. W. Grant, Phys. Rev. Lett. **20**, 1279 (1968).
[6]R. M. Housley, R. W. Grant, and U. Gonser, Phys. Rev. **178**, 514 (1969).
[7]*Mineral Powder Diffraction File* compiled by the Joint Committee on Powder Diffraction Standards, International Center for Diffraction Data, Swarthmore, PA, 19801, p. 887 (unpublished).
[8]W. A. Deer, R. A. Howie, and J. Zussman in *Rock Forming Minerals* (Wiley, New York, 1964), Vol. 5, p. 273.
[9]W. E. Sharp, Am. Mineral. **45**, 241 (1960).
[10]See U.S. Patent 5 327 733 (issued July 12, 1994) that describes the mounting method. P. Boolchand, G. H. Lemon, W. J. Bresser, R. N. Enzweiler, and R. L. Harris (unpublished). Also see Y. Wu, S. Pradhan, and P. Boolchand, Phys. Rev. Lett. **67**, 3184 (1991).
[11]M. Blume and O. C. Kistner, Phys. Rev. **171**, 417 (1968).
[12]G. T. Trammell, Phys. Rev. **126**, 1045 (1962).
[13]P. Boolchand, Ph.D. thesis Case Western Reserve University, 1969; see also P. Boolchand. B. L. Robinson, and S. Jha, Phys. Rev. B **2**, 3463 (1970).